JOURNAL OF THEORETICAL
AND APPLIED MECHANICS
1, **40**, 2002

RELIABILITY STUDY OF A CONTAINMENT SHELL

Eligiusz Postek
Andrzej Siemaszko
Institute of Fundamental Technological Research, Warsaw
e-mail: epostek@ippt.gov.pl

Michał Kleiber
Institute of Fundamental Technological Research, Warsaw
Faculty of Mathematics and Information Science, Warsaw University of Technology
e-mail: mkleiber@ippt.gov.pl

Computational time needed for reliability analysis of realistic structural problems as a rule is very high. Improvements in efficiency are critical to allow solution of large realistic problems. The reliability analysis is usually performed using approximate First Order Reliability Method (FORM). Iterative solution procedures of FORM require extensive design sensitivity computations of high accuracy. The design of realistic structures requires computer-based numerical procedures, such as finite element analysis. The design sensitivity gradients are not explicitly available in terms of design variables. The most intensive computational task of design sensitivity computation should be carried out by highly efficient and accurate methods such as discrete design sensitivity analysis. This paper describes requirements for design sensitivity information for reliability analysis. The way of coupling reliability computation with discrete AVM and DDM methods of design sensitivity analysis is pointed out. A computational program developed for layered concrete shells allows one to solve large realistic reliability problems. The reliability study of an RC nuclear containment shell is carried out. Reliability studies show which of the parameters have the highest impact on the reliability of the vessel.

Key words: nuclear engineering, reliability, design sensitivity, FEM

1. Introduction

Design of advanced structural systems should account for randomness of geometric, material and loading parameters. Furthermore, the reliability should be evaluated as the most objective structural safety measure. Computational time for reliability analysis of realistic structural problems is very high. Improvements in efficiency are critical to allow solution of large realistic problems.

The reliability analysis is usually performed using approximate First Order Reliability Method (FORM). Iterative solution procedures of FORM require substantial design sensitivity computations of high accuracy. The design of realistic structures requires computer-based numerical procedures, such as finite element analysis. For these structures, sensitivity is not available explicitly in terms of design variables. The most intensive computational task of design sensitivity computation is often carried out quite inefficiently by the finite difference method. It is obvious, that to increase efficiency and accuracy of FORM procedures the continuum or discrete methods of design sensitivity analysis instead of the finite difference one should be used.

This paper shows that integration of discrete sensitivity analysis method with reliability analysis may produce an efficient system allowing one to solve large realistic design problems. The paper describes requirements for design sensitivity information and points out the way of coupling reliability computation with design sensitivity analysis. Practical developments are concentrated on layered shells.

A reliability study of the containment structure is performed. Componental reliability indices and the design derivatives of the indices with respect to design parameters are calculated. Reliability studies show which parameters have the highest impact on the reliability of the containment.

2. Reliability analysis

The first step in evaluating the reliability of a structure is usually the identification of a number of variables by which the uncertainties related to the structural system can be described satisfactorily. They are called basic variables and are modelled as random variables or, if necessary, as stochastic processes.

Let $\boldsymbol{X} = \{X_1, X_2, \ldots, X_n\}^\top$ be the vector of random variables. Specific realization of the vector $\boldsymbol{X}$ is denoted by $\boldsymbol{x} = \{x_1, x_2, \ldots, x_n\}^\top$. It is useful to consider the variable $\boldsymbol{x}$ as a point in an n-dimensional basic variable space Ω. The number of basic variables n is assumed finite. For a given set of realizations of random variables, $\boldsymbol{x}$, it is assumed that it is possible to determine whether the structure is in a failure state or in a safe state. In other words, the random variable space Ω is divided into two sets called the failure domain Ω_f and the safe domain Ω_s. The hypersurface separating the two domains Ω_f and Ω_s is called the failure surface and it is described by a failure function $g(\boldsymbol{x}) = 0$ defined in such a way that positive value of g corresponds to the safe domain and non-positive value of g to the failure domain, i.e.

$$\begin{aligned} g(\boldsymbol{x}) > 0 \qquad & \text{when} \quad \boldsymbol{x} \in \Omega_s \\ g(\boldsymbol{x}) \leqslant 0 \qquad & \text{when} \quad \boldsymbol{x} \in \Omega_f \end{aligned} \tag{2.1}$$

The probability of failure describes the probability that the limit (failure) state will be attained, i.e. $g(\boldsymbol{x})$ will be less or equal to zero. This is given by

$$p_f = P[g(\boldsymbol{X}) < 0] = \int\limits_{g(\boldsymbol{x})\leqslant 0} f_X(\boldsymbol{x})\, dx \tag{2.2}$$

where $f_X(\boldsymbol{x})$ is the joint probability density function of $\boldsymbol{X}$.

The integration is performed over the failure region Ω_f. If some of the basic random variables are discrete, the integration over the corresponding densities is substituted by a summation over finite probabilities.

The reliability analysis aims at evaluation of the multidimensional integral in Eq. (2.2). Only a few analytical and exact results are known. Standard numerical integration techniques are generally not feasible for high-dimensional problems, and in general, either Monte Carlo simulation (MCS), or the analytically based first- and second-order reliability methods (FORM/SORM) must be used.

The methods, MCS and FORM/SORM should be considered as complementary methods. For example, if the basic variables are discrete, the necessary transformation between the physical x-space and the standard normal u-space does not exist and MCS methods must be used.

In FORM method the failure function $g(\boldsymbol{u}) = 0$ is expanded up to the first order at the β-point (Madsen et al., 1986; Hasofer and Lind, 1974). This is defined as the point on $g(\boldsymbol{u}) = 0$ at the shortest distance from the origin of the coordinate system to the linearized failure surface in the standardized normal space. Reliability index corresponding to the β-point is evaluated by the minimization problem

$$\beta = \|\boldsymbol{u}^\star\| = \min \|\boldsymbol{u}\| \qquad \text{subject to} \quad g(\boldsymbol{u}) = 0 \tag{2.3}$$

The β-point should be defined in the normal space. Several methods for reaching β-point have been developed and the R-F algorithm is one of them, Ref. [19].

3. Requirements for design sensitivity information

Accounting for complex reliability models in the design/optimization problems requires that effective and accurate sensitivity analysis of the structural performances measures with respect to design parameters can be realised. Especially, if general nonlinear optimization algorithms are used, high precision sensitivity coefficients are needed in order to assure convergence. This paper presents a strategy for integration of reliability analysis with the discrete design sensitivity analysis (DSA). The potential failure mode is described by the failure function

$$g\{(\boldsymbol{x}(\boldsymbol{u}), \Psi[\boldsymbol{x}(\boldsymbol{u})]\} = 0 \tag{3.1}$$

where Ψ is a general performance measure, e.g., a componental stress or a nodal displacement component and $\boldsymbol{x}$ is the vector of realizations of random variables. Solution to Eq. (2.3) requires the computation of the first derivative of the failure function, Eq. (3.1), with respect to the standard variables $\boldsymbol{u}$

$$\frac{dg}{d\boldsymbol{u}} = \frac{\partial g}{\partial \boldsymbol{x}} \frac{\partial \boldsymbol{x}}{\partial \boldsymbol{u}} + \frac{\partial g}{\partial \Psi} \frac{\partial \Psi}{\partial \boldsymbol{x}} \frac{\partial \boldsymbol{x}}{\partial \boldsymbol{u}} \tag{3.2}$$

The derivatives $\partial g/\partial \Psi$ and $\partial g/\partial \boldsymbol{x}$ are given explicitly. The advanced reliability codes compute the derivatives $\partial \boldsymbol{x}/\partial \boldsymbol{u}$ internally from the transformation $\boldsymbol{x} = T(\boldsymbol{u})$. The most difficult and time consuming task is to compute derivatives of the performance measure w.r.t. $\partial \Psi/\partial \boldsymbol{x}$. This is performed by highly efficient adjoint variable method of DSA (Madsen et al., 1986). For structural safety considerations it is important to have capabilities for performing reliability parametric studies. Then, it is necessary to compute the derivatives of the reliability index β w.r.t design parameters $\boldsymbol{x}^\mu$ and $\boldsymbol{x}^\sigma$ assigned to mean values and standard deviations of random parameters, respectively, as well as to deterministic design parameters $\boldsymbol{x}^d$. The following formulae should be used

$$\frac{d\beta}{d\boldsymbol{x}^\alpha} = \left\| \frac{\partial g}{\partial \boldsymbol{u}} \right\|^{-1} \frac{\partial g}{\partial \boldsymbol{x}^\alpha} \frac{\partial T}{\partial \boldsymbol{u}} \qquad \text{for} \quad \boldsymbol{x}^\alpha = \boldsymbol{x}^\mu, \boldsymbol{x}^\sigma \tag{3.3}$$

where the gradients $\partial g/\partial \boldsymbol{x}^\alpha$, $\partial g/\partial \boldsymbol{u}$ and $\partial T/\partial \boldsymbol{u}$ are known from the reliability computations, whereas in the case of deterministic parameters $\boldsymbol{x}^d$

$$\frac{d\beta}{d\boldsymbol{x}^d} = \left\| \frac{\partial g}{\partial \boldsymbol{u}} \right\|^{-1} \frac{\partial g}{\partial \boldsymbol{x}^d} + \frac{\partial g}{\partial \Psi} \frac{\partial \Psi}{\partial \boldsymbol{x}^d} \tag{3.4}$$

where the derivatives $\partial \Psi/\partial \boldsymbol{x}^d$ are also computed by the adjoint variable method of DSA (Ditlevsen and Madsen, 1996).

4. Design sensitivity analysis of layered shells

4.1. Adjoint variable method

Reliability considerations of a nuclear reactor containment shell will be based upon displacement failure functions. To obtain the displacement sensitivities the adjoint variable method of DSA will be employed. The computational aspects of DSA are given in Haug et al. (1986), Kleiber et al. (1997).

Note, that two different displacement sensitivities are required, namely, with respect to realizations of random parameters $\boldsymbol{x}$, Eq. (3.2), and with respect to design parameters $\boldsymbol{x}^\alpha$, Eq. (3.4). From the point of view of DSA this distinction is irrelevant and the computation is exactly the same. Therefore, the sensitivities with respect to design parameters are described.

For the design sensitivity analysis the adjoint variable and direct differentiation methods can be used, Haug et al. (1986). To obtain the displacement failure function sensitivities for the reliability analysis the adjoint variable method is employed and is presented briefly. The equilibrium equation is written as

$$\mathsf{K}\boldsymbol{q}(\boldsymbol{x}^\alpha) = \boldsymbol{Q}(\boldsymbol{x}^\alpha) \tag{4.1}$$

where K is the stiffness matrix, $\boldsymbol{q}$ is the displacement vector, and $\boldsymbol{Q}$ is the external load vector. All these quantities depend on the design parameters $\boldsymbol{x}^\alpha$ comprising the deterministic parameters $\boldsymbol{x}^d$ and mean values $\boldsymbol{x}^\mu$ of the random parameters $\boldsymbol{X}$. Sensitivity of the performance measure Ψ, where $\Psi = \Psi(q(\boldsymbol{x}^\alpha), \boldsymbol{x}^\alpha)$, with respect to the design parameter $\boldsymbol{x}^\alpha$ can be written as

$$\frac{d\Psi}{d\boldsymbol{x}^\alpha} = \frac{\partial\Psi}{\partial\boldsymbol{x}^\alpha} - \boldsymbol{\lambda}^\top\Big(\frac{\partial\mathsf{K}}{\partial\boldsymbol{x}^\alpha}\boldsymbol{q} - \frac{\partial\boldsymbol{Q}}{\partial\boldsymbol{x}^\alpha}\Big) \tag{4.2}$$

where $\boldsymbol{\lambda}$ is obtained from the adjoint equation

$$\mathsf{K}\boldsymbol{\lambda} = \Big(\frac{\partial\Psi}{\partial\boldsymbol{q}}\Big)^\top \tag{4.3}$$

As design parameters for the layered shell element the Young modulus, thickness of the reinforcement layer and its position with respect to the midsurface are considered. As performances the displacements are considered.

In contrast to the known commercial FEA programs like Nastran [20], Abaqus [18] where the design derivatives are calculated using finite difference method, which may lead to a dependence of the results on the selected perturbation, the stiffness design derivatives are calculated explicitly herein.

The explicit expressions for the stiffness design derivatives in Eq. (4.2) for the element considered are given in the subsequent sections.

4.2. Ahmad-type finite element

In application to nuclear reactor containments the isoparametric layered shell element of Ahmad is used (Postek, 1996; Postek and Kleiber, 1996).

To have a consistent derivation, firstly the stiffness matrix of the element is presented, secondly, the contribution of the reinforcement to the element stiffness is shown and finally the design derivatives of the total stiffness matrix, with respect to the design parameters connected with the reinfocement properties, e.g. Young's moduli, thickness and the distance of the reinforcement layer from the midsurface of the shell are presented.

To describe the geometrical relations in the described element four reference sytems are defined, see Fig. 1.

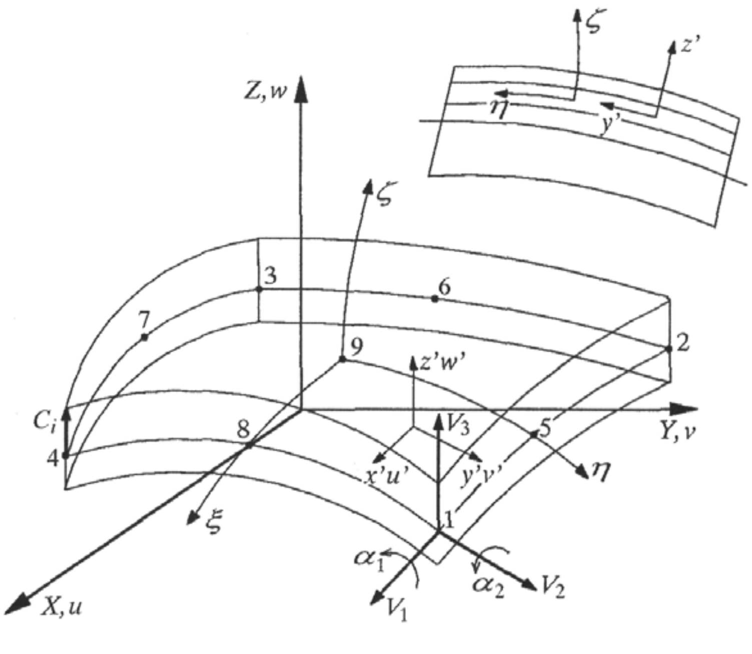

Fig. 1. Layered shell element, coordinate systems

1. Global system – this is an arbitrary Cartesian system $\{X, Y, Z\}$, the final total stiffness is defined in that system.

2. Local isoparametric system ξ, η, ζ – the curved midsurface of the element (in the ξ, η coordinates) and the positions of the layers (by the coordinate) are defined.

3. Local nodal coordinate systems – these systems are defined in each node by three orthogonal vectors $\boldsymbol{V}_1^i, \boldsymbol{V}_2^i, \boldsymbol{V}_3^i$ where i is the node number $i = 1, ..., 9$.

4. Local coordinate system x', y', z' – this is a Cartesian system in which the strains, stresses, generalized forces and the design derivatives are calculated. That system is defined at the integration stations.

The geometry of the element is defined as follows

$$\begin{bmatrix} x \\ y \\ z \end{bmatrix} = \sum_{i=1}^{n} N_i \begin{bmatrix} x_i \\ y_i \\ z_i \end{bmatrix} + \sum_{i=1}^{n} N_i \zeta \frac{t_i}{2} \boldsymbol{V}_3^i \tag{4.4}$$

The displacement field in the element is defined by the following equation

$$\begin{bmatrix} u \\ v \\ w \end{bmatrix} = \sum_{i=1}^{9} N_i \begin{bmatrix} u_i \\ v_i \\ w_i \end{bmatrix} + \sum_{i=1}^{9} N_i \zeta \frac{t_i}{2} \boldsymbol{\Phi}_i \begin{bmatrix} \alpha_{1i} \\ \alpha_{2i} \end{bmatrix} \tag{4.5}$$

where N_i are the Lagrange shape functions and $\boldsymbol{\Phi}_i$ is a vector containing vectors tangent to the midsurface defined in the nodal coordinate system as follows

$$\boldsymbol{\Phi}_i = [-\boldsymbol{V}_2, \boldsymbol{V}_1] \tag{4.6}$$

At each node of the element three tanslational degrees of freedom u, v, w parallel to the axes of the global coordinate system X, Y, Z and two rotational degrees of freedom α_1, α_2 being the rotations about the vectors $\boldsymbol{V}_1$ and $\boldsymbol{V}_2$ are defined.

The geometrical relations developed in the local coordinate system are of the form

$$\begin{bmatrix} e_{x'x'} \\ e_{y'y'} \\ e_{x'y'} \\ e_{x'z'} \\ e_{y'z'} \end{bmatrix} = \begin{bmatrix} \dfrac{\partial}{\partial x'} & 0 & 0 \\ 0 & \dfrac{\partial}{\partial y'} & 0 \\ \dfrac{\partial}{\partial y'} & \dfrac{\partial}{\partial x'} & 0 \\ \dfrac{\partial}{\partial z'} & 0 & \dfrac{\partial}{\partial x'} \\ 0 & \dfrac{\partial}{\partial z'} & \dfrac{\partial}{\partial y'} \end{bmatrix} \begin{bmatrix} u' \\ v' \\ w' \end{bmatrix} \tag{4.7}$$

where

$$\begin{bmatrix} u' \\ v' \\ w' \end{bmatrix} = \boldsymbol{\Theta}^{\top} \begin{bmatrix} u \\ v \\ w \end{bmatrix} \qquad \boldsymbol{\Theta} = [\boldsymbol{V}_1, \boldsymbol{V}_2, \boldsymbol{V}_3] \tag{4.8}$$

The above relation constitutes the dependence between the displacements in the global coordinate system X, Y, Z and the local one x', y', z'. Taking into consideration displacement field (4.5) and geometrical relations (4.7) and denoting by $\mathbf{A}$ the following term

$$\boldsymbol{\Theta}^\top \mathbf{J}^{-1} = \mathbf{A} = \begin{bmatrix} A_{11} & A_{12} & 0 \\ A_{21} & A_{22} & 0 \\ 0 & 0 & A_{33} \end{bmatrix} \tag{4.9}$$

where $\mathbf{J}$ is the Jacobian of the transformation between the local coordinate system x', y', z' and the isoparametric one the geometrical relations take the form

$$\boldsymbol{e}' = \mathbf{B}_i \boldsymbol{\Theta}^\top \begin{bmatrix} u_i \\ v_i \\ w_i \end{bmatrix} + \frac{t_i}{2}(\zeta \mathbf{B}_i + \mathbf{D}_i)\boldsymbol{\Theta}^\top \boldsymbol{\Phi}_i \begin{bmatrix} \alpha_{1i} \\ \alpha_{2i} \end{bmatrix} \tag{4.10}$$

The matrices $\mathbf{B}_i$ and $\mathbf{D}_i$ are of the form

$$\mathbf{B}_i = \begin{bmatrix} B_1 & 0 & 0 \\ 0 & B_2 & 0 \\ B_2 & B_1 & 0 \\ 0 & 0 & B_1 \\ 0 & 0 & B_2 \end{bmatrix}_i \qquad \mathbf{D}_i = \begin{bmatrix} 0 & 0 & 0 \\ 0 & 0 & 0 \\ 0 & 0 & 0 \\ D_1 & 0 & 0 \\ 0 & D_1 & 0 \end{bmatrix}_i \tag{4.11}$$

where

$$\begin{aligned} B_1 &= A_{11} N_{i,\xi} + A_{12} N_{i,\eta} \\ B_2 &= A_{21} N_{i,\xi} + A_{22} N_{i,\eta} \\ D_1 &= A_{33} N_i \end{aligned} \tag{4.12}$$

The stiffness matrix is obtained using numerical integration. The element is layered and is integrated using Simpson's rule throughout the thickness and 4 or 9 points Gauss rule over the surface. The ready for programming stiffness matrix is of the form

$$\begin{aligned} \mathbf{K}_E^{ij} &= \sum_{m=1}^{N} \sum_{n=1}^{nc+1} w_m w_n^c \begin{bmatrix} \boldsymbol{\Theta}^\top & \mathbf{0} \\ \mathbf{0} & \frac{t_i}{2}\boldsymbol{\Theta}^\top \boldsymbol{\Phi}_j \end{bmatrix}_m [\mathbf{B}_i | \zeta^z \mathbf{B}_i + \mathbf{D}_i]_m^\top \cdot \\ &\cdot \ \mathbf{C}_{mn}^c \, [\mathbf{B}_j | \zeta^z \mathbf{B}_j + \mathbf{D}_j]_m \begin{bmatrix} \boldsymbol{\Theta}^\top & \mathbf{0} \\ \mathbf{0} & \frac{t_j}{2}\boldsymbol{\Theta}^\top \boldsymbol{\Phi}_j \end{bmatrix} \det \mathbf{J}_m \end{aligned} \tag{4.13}$$

The $\mathbf{C}^c_{mn}$ is the constitutive matrix for the orthotropic material defined at the integration stations, the summation over m is done over integration points; N depending on the integration rule is 4 or 9. The summation over n is done throughout the thickness; nc is the number of the concrete layers in the element, w_m is the Gauss weight, ζ^c_n is the normalized coordinate of the layer n measured in the direction ζ and w^c_n is the weighting coefficient for the Simpson rule; t_m is the thickness of the shell at the point m.

4.3. Reinforcement

The 'smeared' model of the reinforcement is used. The equivalent thickness $t_s = A_s d$, where A_s is the cross-sectional area of the reinforcement bar and d is the distance between the bars, is assumed. The uniaxial stress state is assumed in the reinforcing bars. The reinforcement is assumed to be placed in two orthogonal directions. Then, the constitutive matrix for the reinforcement assuming its existence in both directions is of the form

$$\mathbf{C}'_s = \begin{bmatrix} E_s & 0 & 0 & 0 & 0 \\ & E_s & 0 & 0 & 0 \\ & & 0 & 0 & 0 \\ & & & 0 & 0 \\ & & & & 0 \end{bmatrix} \tag{4.14}$$

If the reinforcement exists only in one chosen direction the nonzero elements of the above matrix (4.14) are the relevant , $C'_{s(11)} = E_s$ or $C'_{s(22)} = E_s$ terms (E_s is the Young modulus for the reinforcement). The total stiffness is the sum of the stiffness of the concrete and the equivalent reinforcement layers

$$\mathbf{K}_E = \mathbf{K}_c + \mathbf{K}_s \tag{4.15}$$

The stiffness matrix of the reinforcement is similar to the stiffness matrix (4.13) presented above. It is obtained introducing instead of the constitutive matrix for the orthotropic material the relevant constitutive matrices for the equivalent reinforcement layers (4.14). The stiffness matrix for the reinforcement layers is of the form

$$\begin{aligned} \mathbf{K}^{ij}_s \;=\; & \sum_{m=1}^{N}\sum_{n=1}^{ns} w_m w^s_n \begin{bmatrix} \boldsymbol{\Theta}^\top & \mathbf{0} \\ \mathbf{0} & \frac{t_i}{2}\boldsymbol{\Theta}^\top\boldsymbol{\Phi}_i \end{bmatrix}^\top_m [\mathbf{B}_i|\zeta^s\mathbf{B}_i + \mathbf{D}_i]^\top_m \cdot \\ & \cdot\; \mathbf{C}^s_{mn}\,[\mathbf{B}_j|\zeta^s\mathbf{B}_j + \mathbf{D}_j]_m \begin{bmatrix} \boldsymbol{\Theta}^\top & \mathbf{0} \\ \mathbf{0} & \frac{t_j}{2}\boldsymbol{\Theta}^\top\boldsymbol{\Phi}_j \end{bmatrix}_m \det \mathbf{J}_m \end{aligned} \tag{4.16}$$

The summation over m index denotes the sum over the Gauss points on the surface of the element, ns is the number of the reinforcement layers, ζ_n^s is the non-dimensional coordinate fixing the position of the reinforcement layer with respect to the midsurface of the shell element (direction ζ) and $\mathbf{C}_{mn}^s$ is the constitutive matrix of the reinforcement layer at the integration station.

4.4. Design derivatives of the stiffness matrix with respect to the reinforcement parameters

The formulae concerning the design derivatives of the total stiffness matrix with respect to the selected design parameters of the reinforcement such as the Young modulus, thickness of the reinforcement layer and the distance of the reinforcement layer from the midsurface of the shell are presented herein. To calculate the design derivative of the total stiffness at the chosen layer the components of the design derivatives at the reinforcement layer should be calculated and summed up.

In the case of the Young modulus the design derivative takes the form

$$\begin{aligned}\frac{\partial \mathbf{K}_s^{ij}}{\partial E} = & \sum_{m=1}^{N} w_m w_{il}^s \begin{bmatrix} \boldsymbol{\Phi}^\top & \mathbf{0} \\ \mathbf{0} & \frac{t_i}{2}\boldsymbol{\Phi}^\top\boldsymbol{\Phi}_i \end{bmatrix}_m^\top [\mathbf{B}_i|\zeta^s\mathbf{B}_i + \mathbf{D}_i]_m^\top \cdot \\ & \cdot \frac{\partial \mathbf{C}_{m(il)}^s}{\partial E} [\mathbf{B}_j|\zeta^s\mathbf{B}_j + \mathbf{D}_j]_m \begin{bmatrix} \boldsymbol{\Phi}^\top & \mathbf{0} \\ \mathbf{0} & \frac{t_j}{2}\boldsymbol{\Phi}^\top\boldsymbol{\Phi}_j \end{bmatrix} \det \mathbf{J}_m\end{aligned} \tag{4.17}$$

The design derivative of the constitutive matrix (4.14) with respect to the Young modulus in the case of the existence of reinforcement in both orthogonal directions is of the form

$$\frac{\partial \mathbf{C}_{m(il)}^s}{\partial E} = \begin{bmatrix} 1.0 & 0 & 0 & 0 & 0 \\ & 1.0 & 0 & 0 & 0 \\ & & 0 & 0 & 0 \\ & & & 0 & 0 \\ & & & & 0 \end{bmatrix} \tag{4.18}$$

If the reinforcement exists only in one selected direction the relevant elements of the matrix given above are zeroed (element 11 or element 22).

The formula for the design derivative of the total stiffness matrix with respect to the thickness of the reinforcement layer is obtained by differentiating formula (4.13) with respect to the thickness of the layer at each integration station in the layer. The component of the stiffness matrix connected with the reinforcement layer in the element is linearly dependent on the weighting factor of the rectangular integration rule. In consequence, the design derivative of the total stiffness w.r.t the thickness of the particular layer takes the form

$$
\begin{aligned}
\frac{\partial \mathbf{K}_s^{ij}}{\partial t_s} &= \sum_{m=1}^{N} w_m \frac{2}{t_m} \begin{bmatrix} \boldsymbol{\Phi}^\top & \mathbf{0} \\ \mathbf{0} & \frac{t_i}{2}\boldsymbol{\Theta}^\top \boldsymbol{\Phi}_i \end{bmatrix}_m^\top [\mathbf{B}_i | \zeta^s \mathbf{B}_i + \mathbf{D}_i]_m^\top \cdot \\
&\cdot \ \mathbf{C}^s_{m(il)} \, [\mathbf{B}_j | \zeta^s \mathbf{B}_j + \mathbf{D}_j]_m \begin{bmatrix} \boldsymbol{\Phi}^\top & \mathbf{0} \\ \mathbf{0} & \frac{t_j}{2}\boldsymbol{\Theta}^\top \boldsymbol{\Phi}_j \end{bmatrix}_m \det \mathbf{J}_m
\end{aligned}
\tag{4.19}
$$

Finally, in the case of the distance of the reinforcement layer from the mid-surface of the shell the design derivative of the stiffness matrix with respect to that parameter is of the form

$$
\begin{aligned}
\frac{\partial \mathbf{K}_s^{ij}}{\partial \zeta^{il}} &= \sum_{m=1}^{N} w_m w_{il}^s \begin{bmatrix} \boldsymbol{\Phi}^\top & \mathbf{0} \\ \mathbf{0} & \frac{t_i}{2}\boldsymbol{\Theta}^\top \boldsymbol{\Phi}_i \end{bmatrix}_m^\top \cdot \\
&\cdot \begin{bmatrix} 0 & 0 & 0 & b_{11}E_s^{(il)} & 0 & 0 \\ 0 & b_{22}E_s^{(il)} & 0 & 0 & b_{22}E_s^{(il)} & 0 \\ 0 & 0 & 0 & 0 & 0 & 0 \\ b_{11}E_s^{(il)} & 0 & 2\zeta^{(il)} b_{12}E_s^{(il)} & 0 & 0 & \\ 0 & b_{22}E_s^{(il)} & 0 & 0 & 2\zeta b_{22} & 0 \\ 0 & 0 & 0 & 0 & 0 & 0 \end{bmatrix}_m \cdot \\
&\cdot \begin{bmatrix} \boldsymbol{\Theta}^\top & \mathbf{0} \\ \mathbf{0} & \frac{t_j}{2}\boldsymbol{\Theta}^\top \boldsymbol{\Phi}_j \end{bmatrix}_m \det \mathbf{J}_m
\end{aligned}
\tag{4.20}
$$

where $b_{11} = B_1^{(i)} B_1^{(j)}$, $b_{22} = B_2^{(i)} B_2^{(j)}$, $b_{12} = B_1^{(i)} B_2^{(j)}$.

The expressions for the stiffness design derivatives can be substituted into Eq. (4.2).

Having the displacement sensitivity field, we may easily obtain the stress sensitivities, considering the formula for strains (4.10), and taking into account the constitutive relations for the reinforcement (4.14), it reads

$$\frac{d\boldsymbol{\sigma}}{dh} = \frac{d\mathbf{C}^s_{m(il)}}{dh} \begin{bmatrix} \boldsymbol{\Phi}^\top & \mathbf{0} \\ \mathbf{0} & \frac{t_j}{2}\boldsymbol{\Theta}^\top \boldsymbol{\Phi}_j \end{bmatrix}_m \boldsymbol{q} + \mathbf{C}_{m(il)} \begin{bmatrix} \boldsymbol{\Phi}^\top & \mathbf{0} \\ \mathbf{0} & \frac{t_j}{2}\boldsymbol{\Theta}^\top \boldsymbol{\Phi}_j \end{bmatrix}_m \frac{d\boldsymbol{q}}{dh} \tag{4.21}$$

The h are the design parameters of the reinforcement (Young's moduli). The stress derivatives with respect to the design parameters of the concrete matrix can be obtained setting the constitutive matrix for the orthotopic material in formula (4.21).

4.5. Design derivatives validation

As a testing example a hypar structure is chosen, Figure 2. The standard equlibrium analysis was done by several authors and the results are well documented in the literature, Chetty and Tottenham (1964), Connor and Brebbia (1967), therefore that structure is also considered by us as a benchmark for the DSA.

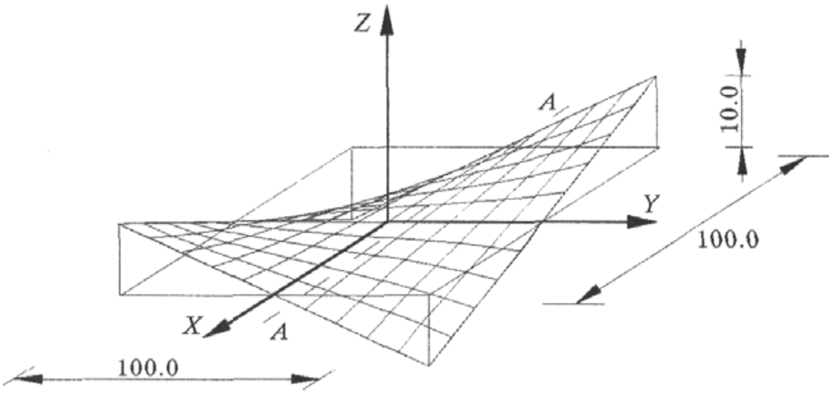

Fig. 2. Hypar, geometry and the discretization

The following material data are assumed (non-dimensional): Young's modulus 28500, Poisson's coefficient 0.4, thickness of the shell 0.8. The shell is reinforced with two orthotropic reinforcement layers. The distances of the layers measured in the isoparametric coordinates are ± 0.555. Young's modulus of the reinforcement is 2.5×10^6. The equivalent thickness of the reinforcement is 0.065. The shell is fixed on its edges and is loaded with the unit pressure normal to the midsurface. The structure is meshed with 100 elements.

The design sensitivity gradients are obtained using the adjoint variable method (AVM) and are verified with finite differences. The design sensitivity

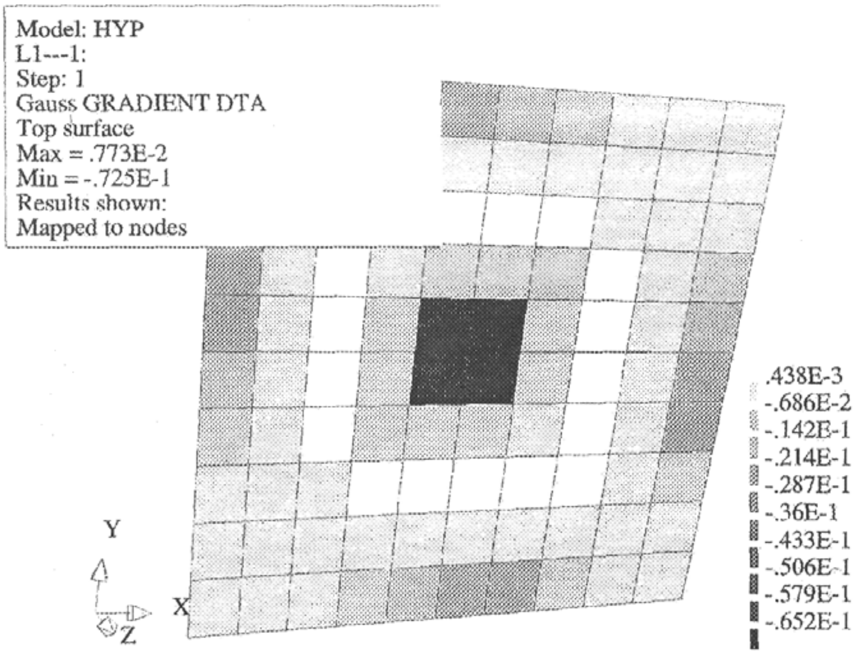

Fig. 3. Design sensitivity of the vertical displacement of the midpoint of the structure w.r.t the distances of the lower reinforcement layer

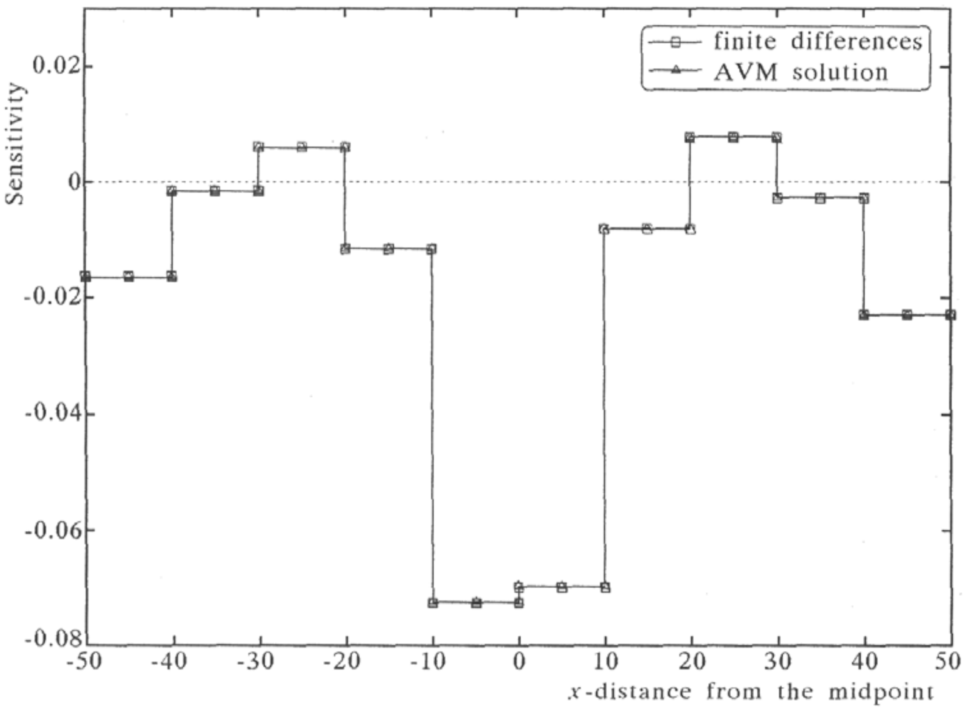

Fig. 4. Design sensitivity of the vertical displacement of the midpoint of the structure w.r.t the distances of the lower reinforcement layer in particular elements along the line $A - A$ computed by finite differences and AVM

of the vertical displacement of the midpoint of the structure with respect to the distances of the lower reinforcement layer in particular elements is investigated.

The distribution of the design sensitivity gradients is presented in Figure 3. The highest absolute values of the sensitivity gradients are in the midpoint area of the structure which means that the perturbation of the distance from the midsurface of the shell in the investigated reinforcement layer influences the considered displacement the most.

Further, the design sensitivity gradients (along the line $A - A$, Fig. 2) are compared with the one obtained with finite differences. The results are presented in Figure 4. The difference between the gradients obtained by both methods does not exceed 1.12% with the perturbation 0.99%.

5. Reliability study of the concrete containment shell

In the event of a severe accident, the pressure inside a containment building may significantly exceed the postulated design pressure. Since the containment structure provides the last structural barrier against the leakage of a radioactive material into the environment in the event of beyond-design-basis accident, knowledge of performance of the containment structure subjected to internal pressure associated with the accident is essential.

The reliability analysis (RA) associated with reliability sensitivity analysis (RSA) constitutes an effective investigative tool to supplement but not at all to replace the traditional deterministic approach. The RA/RSA not only grants a quantitative perspective on the plant safety but also provides a more balanced, objective and realistic picture. The most important results provided are engineering insights, i.e. the identification of vulnerabilities to a high safety level of the plant, sensitivities of reliability measures with respect to design parameters and the assessment of alternative means for improvements.

As an example a reliability study of a reinforced concrete nuclear containment shell is presented. The geometry of the structure and a typical cross-section of the wall are presented in Figure 5. The structure consists of the cylinder (radius 20 m) and the dome (radius 20 m). The height of the structure is 64 m. In this example the stochastic parameters are connected with the reinforcement layers system and internal pressure. The goal of the analysis is to evaluate the reliability of the system considering a displacement failure function corresponding with the appearance of the first crack in concrete. The structure is discretized with 640 shell elements, Figure 6. The number of degrees of freedom is about 12500. The cylindrical and the dome parts of

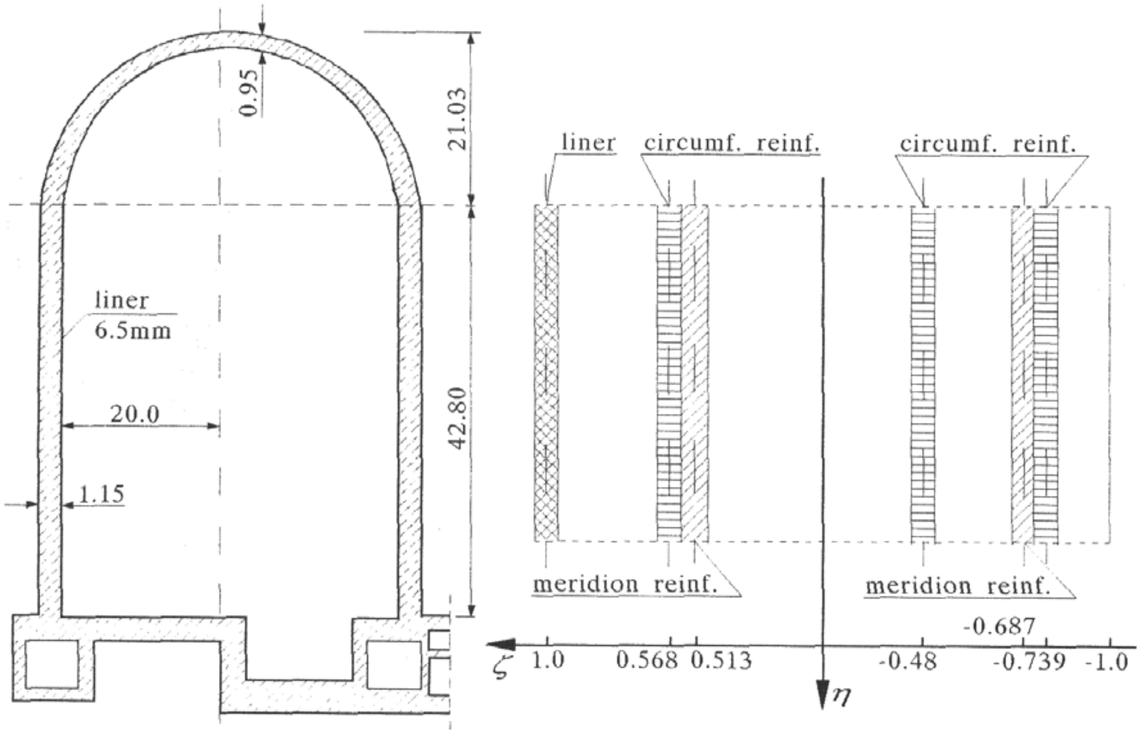

Fig. 5. The vertical cross-section of the structure

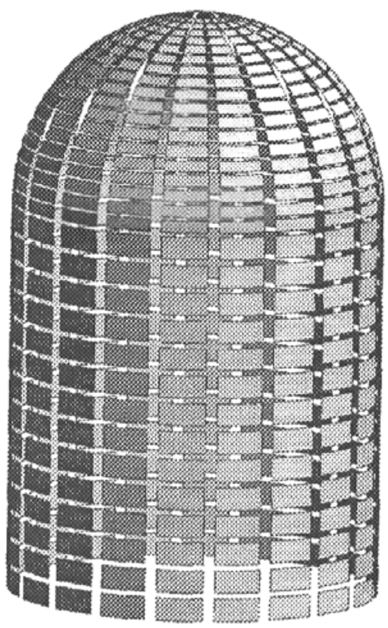

Fig. 6. Finite element discretization, shrink plot

the vessel are prestressed by a system of tendons. The action of tendons is approximated by an external pressure. The aspects of the standard stress-displacement deterministic analysis were presented in Barbat et al. (1995), Postek et al. (1994).

To perform the reliability study of the structure, the reliability analysis code COMREL (Hasofer and Lind, 1974; Ditlevsen and Madsen, 1996), has been integrated with the finite element code POLSAP-RC for analysis of layered shells. Design sensitivity capabilities have been added, as described in Section 4 (Postek, 1996; Postek and Kleiber, 1996).

As variable design parameters the mean values of the thicknesses of the equivalent steel layers, distances of the reinforcement from the midsurface of the shell and the load multipliers are considered, see Table 1. The reinforcement placement and the geometric data are shown in Figure 7 and Table 1, respectively. The data concerning the internal pressure distribution are taken after Postek et al. (1994). However, we investigate the first crack pressure. For the internal pressure the log-normal distribution with a standard deviation equal to 20% has been assumed. In our specific case the stochastic model consists of 3841 parameters. The parameters connected with the structure are the thicknesses of the particular reinforcement equivalent layers and their distances from the midsurface of the shell in particular finite elements. The parameters characterize the errors of the reinforcement distribution and placement.

Table 1. Reinforcement parameters

Zone	Distance from midsurface	Equivalent thickness	Description
I	1.000	0.650E−2	liner
	−0.739	0.761E−2	circ. ext.
	0.513	0.264E−2	circ. internal
	−0.687	0.940E−2	meridional ext.
	0.565	0.974E−2	meridional internal
	−0.480	0.900E−2	prestressed (circ.)
II	1.000	0.650E−2	liner
	−0.739	0.761E−2	circ. ext.
	0.513	0.264E−2	circ. internal
	−0.687	0.530E−2	meridional ext.
	0.565	0.309E−2	meridional internal
	−0.480	0.900E−2	prestressed (circ.)

III	1.000	0.650E−2	liner
	−0.739	0.761E−2	circ. ext.
	0.513	0.264E−2	circ. internal
	−0.687	0.530E−2	meridional ext.
	0.565	0.193E−2	meridional internal
	−0.480	0.900E−2	prestressed (circ.)
IV	1.000	0.650E−2	liner
	−0.739	0.761E−2	circ. ext.
	0.513	0.264E−2	circ. internal
	−0.687	0.414E−2	meridional ext.
	0.565	0.193E−2	meridional internal
	−0.480	0.900E−2	prestressed (circ.)
V	1.000	0.650E−2	liner
	−0.725	0.471E−2	circ. ext.
	0.537	0.275E−2	circ. internal
	−0.725	0.448E−2	meridional ext.
	0.537	0.217E−2	meridional internal
	−0.480	0.900E−2	prestressed (circ.)
VI	1.000	0.650E−2	liner
	−0.725	0.328E−2	circ. ext.
	0.537	0.204E−2	circ. internal
	−0.725	0.328E−2	meridional ext.
	0.537	0.204E−2	meridional internal
	−0.480	0.900E−2	prestressed (circ.)
VII	1.000	0.650E−2	liner
	−0.725	0.328E−2	circ. ext.
	0.537	0.275E−2	circ. internal
	−0.725	0.328E−2	meridional ext.
	0.537	0.217E−2	meridional internal
	−0.480	0.900E−2	prestressed (dome)

We have assumed a Gaussian distribution of the thicknesses and distances of the layers. The assumed values of the standard deviations for the thicknesses are as follows (layerwise): 15%, 15%, 1.5%, 15%, 15%, 16%, and for the distances from the midsurface 0.8%, 0.4%, 0.5%, 0.5%, 0.1% and 0.5%.

As the potential failure mode the gross structural failure of the containment structure is considered. From the deterministic studies the critical horizontal displacement q^* in the middle of the cylindrical wall is assumed and the associated actual displacement q taken as a representative of the overall containment deformation.

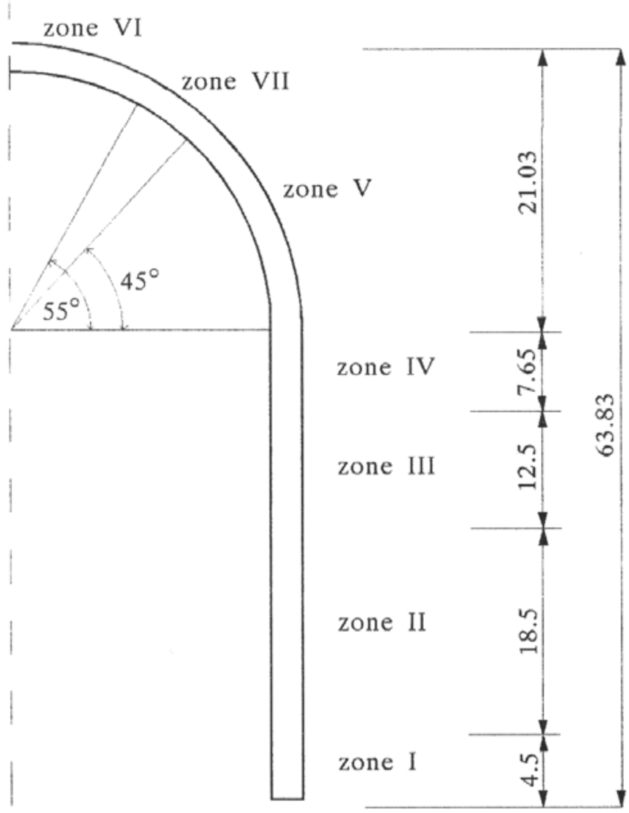

Fig. 7. Reinforcement zones

The global failure function is described by an excessive displacement

$$g(x) = q^{\star} - q \tag{5.1}$$

where $q^{\star}$ is the admissible displacement corresponding to the first crack occurence. It is equal to 0.15E−2 m. The displacement is caused by the deterministic internal pressure $756\,\mathrm{kN/m^2}$.

We have started the analysis for the internal pressure far below its first crack value i.e. for the load multiplier equal to 6.5. For that pressure when considering the layer thicknesses as the design parameters the β index is 6.08 with the corresponding probability $p_f = 6.17\mathrm{E} - 10$ and when taking into account the distances of the reinforcement from the midsurface of the shell the β index and the probability of failure are 6.11 and 4.93E−10, respectively.

We will not deal with the description of the establishing the critical displacement since it is beyond the scope of the considerations, it is possible to obtain the first crack value by any method concerning the first crack criterion assuming linear, in that case, behaviour of the materials and the geometry of the structure.

Table 2. Reliability indices and the corresponding probabilities of reaching the design constraint

Internal pressure factor	Rel. index (thickness of layers)	Probability (thickness of layers)	Rel. index (distance of of layers)	Probability (distance of layers)	Considered displacement [m]
6.5	6.0764	6.1685E-10	6.1122	4.9316E-10	0.4824E-03
6.6	5.1342	1.4193E-07	5.1639	1.2114E-07	0.5766E-03
6.7	4.3157	7.9589E-06	4.3418	7.9589E-06	0.6727E-03
6.8	3.6263	1.4308E-04	3.6509	1.3970E-04	0.7688E-03
6.9	2.9800	1.4411E-03	3.0026	1.3383E-03	0.8648E-03
7.0	2.4354	7.4380E-03	2.4576	6.9938E-03	0.9648E-03
7.1	1.9705	2.4388E-02	1.9934	2.3108E-02	0.1057E-02
7.2	1.4583	7.2375E-02	1.4792	6.9544E-02	0.1158E-02
7.3	1.0880	0.1383	1.1127	0.1329	0.1254E-02
7.4	0.6569	0.2556	0.6796	0.2484	0.1345E-02
7.5	0.2833	0.3885	0.3042	0.3805	0.1414E-02
7.55	0.0990	0.4606	0.9902E-01	0.4606	0.1489E-02

The reliability analysis is performed varying the internal pressure factor. The numerical results are collected in Table 2 and presented in Figure 8.

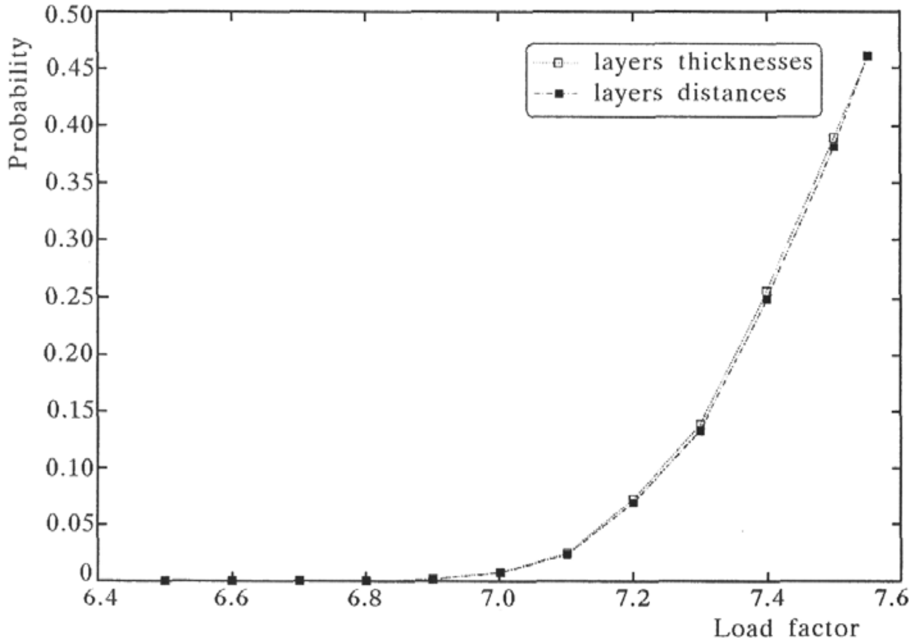

Fig. 8. Probability of the failure versus load level (displacement constraint)

The dependence of probability of failure (i.e. violation of the condition (5.1)) versus internal pressure factor is given in Fig. 8. The probabilities of failure starts to increase significantly after passing the internal load pressure factor 7.0.

Further, the design derivatives fields for the load level causing the displacement close to the established failure condition are presented. Figure 9 shows the design sensitivity of the selected displacement with respect to the thicknesses of the external circumferential reinforcement in particular elements at the pressure close to the first crack pressure (AVM method). The displacement derivative field with respect to the thickness of the external circumferential layer in element 165 (close to the midspan of the cylinder) is presented in Figure 10. The direct differentiation method (DDM) is used, details of the method are not presented since it is used only for the deterministic analysis herein.

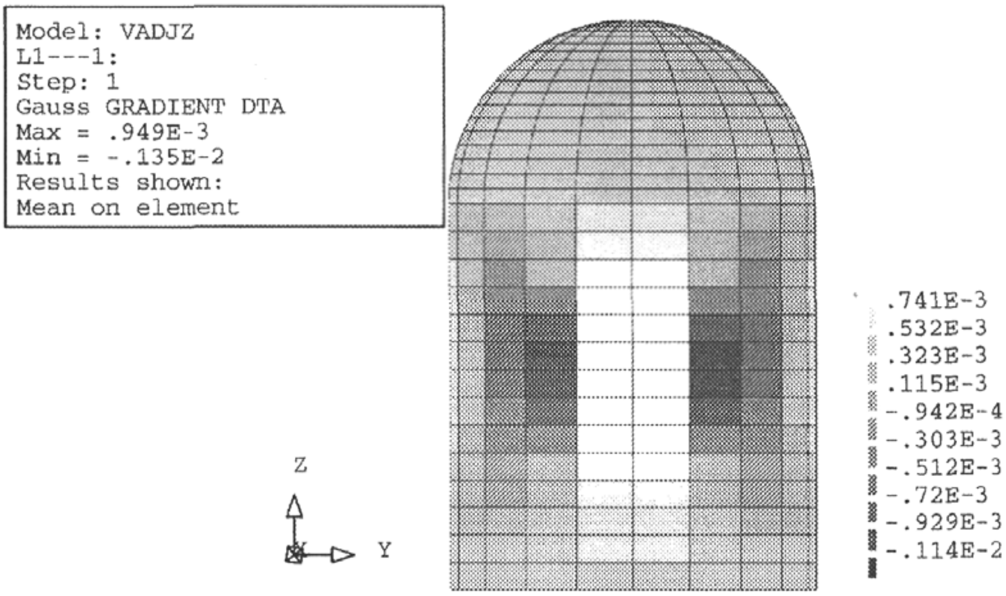

Fig. 9. Design sensitivity of the selected displacement with respect to the thickness of external circumferential reinforcement

Figure 11 shows the distribution of the circumferential stress derivative field (in the external concrete layer) with respect to the thickness of the external circumferential layer in element 165.

The following two pictures show the distribution of the reliability index derivatives w.r.t. the distances of the external circumferential layer in particular elements (mean values and standard deviations) (Figures 12 and 13).

Further, a numerical experiment is performed assuming a higher value of the standard deviation of the load multiplier (40%) at the mean value 7.4. Assuming that the stochastic variables are the layers thicknesses the reliability

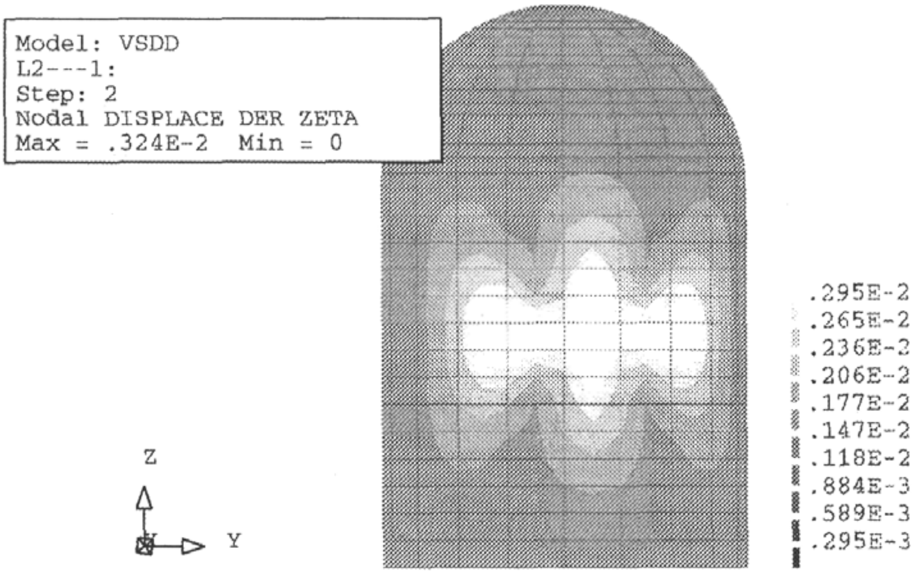

Fig. 10. Displacement derivative field w.r.t the thickness of the external circumferential layer in element 165

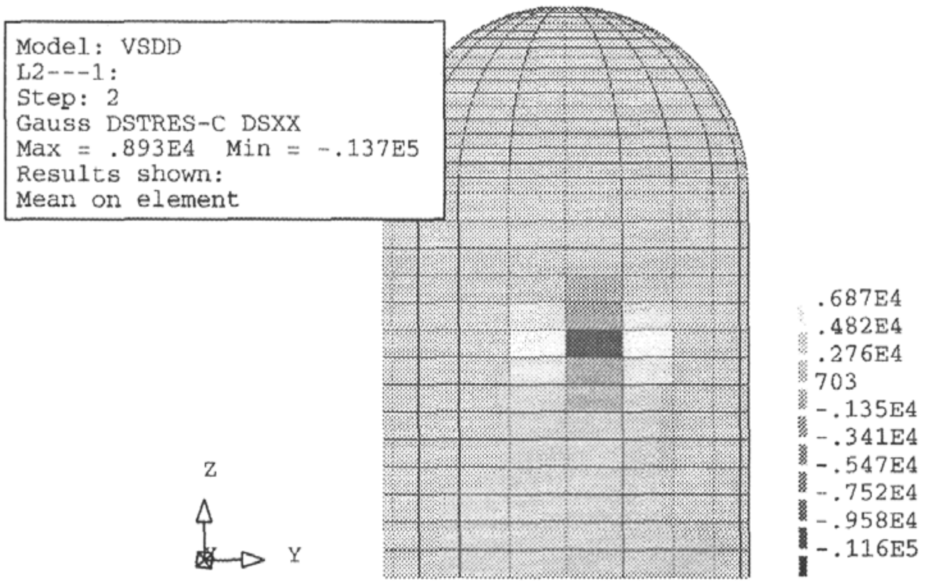

Fig. 11. Circumferential stress derivative field w.r.t. the thickness of the external cicumferential layer in element 165

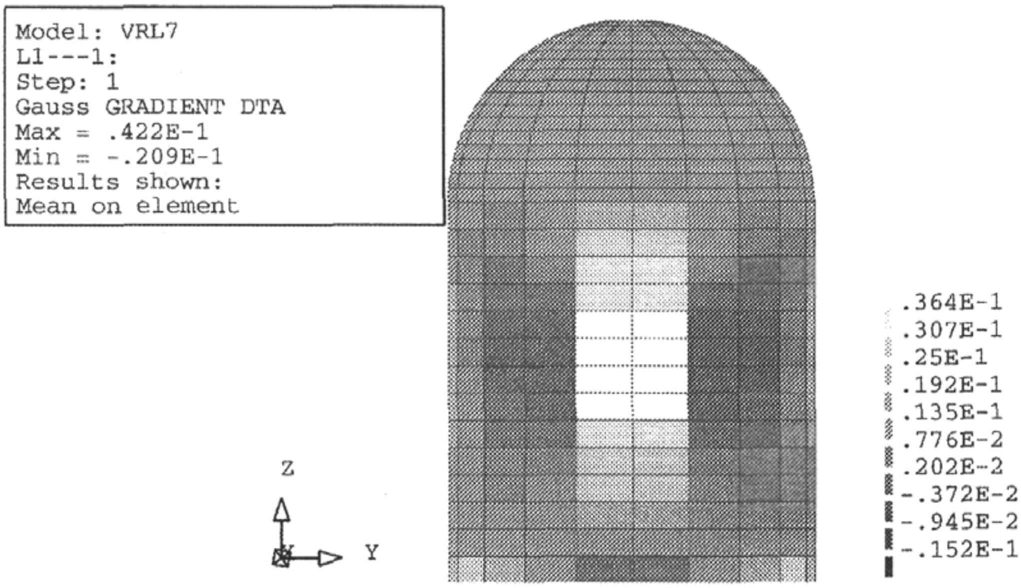

Fig. 12. Beta index derivative field w.r.t the mean values of the distances of the external circumferential layer in particular elements

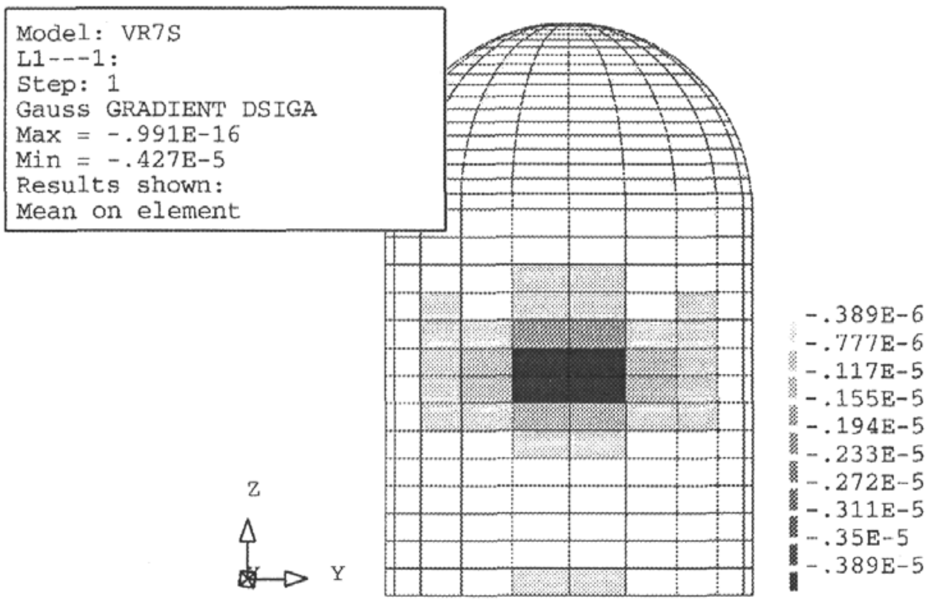

Fig. 13. Beta index derivative field w.r.t the standard deviation of the distances of the external circumferential layer in particular elements

index is 0.4911 and the corresponding probability is 0.3117, when dealing with the layers distances the relevant values are 0.4795 and 0.3158, respectively. In that case the highest impact on the probability of the failure has the load multiplier.

The programs are implemented on the SUN HPC Enterprise 10000 platform. The calculation of the reliability index takes between 1 to 5 hours CPU and the computational time is higher for the high values (close to 6.0) of the reliability index. The run of the reliability module takes only a few per-cent of the total CPU time. The rest is the stress-displacement analysis, the sensitivity gradients calculation takes about 3 minutes of FEA program run. One run of the FEA program takes about 15 minutes for the system considered.

6. Final remarks

This paper put forward a way to integrate the discrete design sensitivity analysis with the reliability analysis and the reliability sensitivity analysis with significant improvement of the computational efficiency. Requirements for design sensitivity information were defined. The adjoint method of discrete design sensitivity analysis was used to derive sensitivity information for the layered reinforcement concrete shell elements. The computational system developed allows are to solve large realistic reliability problems. The reliability study of a reinforced concrete nuclear containment building was carried out.

Acknowledgment

The support from RCP GmbH in Munich, Germany providing the reliability code COMREL is gratefully aknowledged and also the Universidad Politecnica de Catalunya where the idea of the example calculation was risen. The Authors would like also to thank the Interdisciplinary Center for Mathematical Modelling and the Warsaw University of Technology for providing the computer facilities.

References

1. AHMAD S., IRONS B.M., ZIENKIEWICZ O.C., 1970, Analysis of thick and thin shell structures by curved finite elements, *International Journal of Numerical Methods in Engineering*, **2**, 419-451

2. BARBAT A.H., CERVERA M., CIRAUQUI C., HANGANU A., OÑATE E., 1995, Evaluacion de la presion de fallo del edificio de contencion de una central tipo PWR-W tres lazos. Parte II: Simulacion numerica, *Revista International de Met. Num. para Calculo y Diseño en Ingenieria*, **11**, 3, 451-475

3. CHAN E.Y., 1982, Nonlinear geometric, material and time dependent analysis of reinforced concrete shells with edge beams. Technical report, University of California, Berkeley

4. CHETTY S., TOTTENHAM H., 1964, An investigation into the bending analysis of hyperbolic paraboloid shells, *Indian Concrete Jou.*, July

5. CONNOR J.J., BREBBIA C., 1967, Stiffness matrix for shallow rectangular shell element, *J. Eng. Mech. Div., ASCE*, **10**, 43-65

6. DITLEVSEN O., MADSEN H.O., 1996, Structural Reliability Methods, Wiley & Sons

7. HASOFER A.M., LIND N.C., 1974, Exact and invariant second moment code format, *Journal of Engineering Mechanical Division, ASCE*, **100**, 111-121

8. HAUG E.J., CHOI K.K., KOMKOV V., 1986, *Design Sensitivity Analysis of Structural Systems*, Academic Press, New York

9. HOHENBLICHER M., RACKWITZ R., XXXX, First-order concepts in system reliability, *Structural Safety*, **1**, 177-188

10. KLEIBER M., ANTUNEZ H., HIEN T.D., KOWALCZYK P., 1997, *Parameter Sensitivity in Nonlinear Mechanics*, Wiley & Sons

11. MADSEN H.0., KRENK S., LIND N.C., 1986, *Methods of Structural Safety*, Prentice-Hall

12. POSTEK E., 1996, Numerical parameter sensitivity of large nonlinear structural systems, Ph.D. dissertation, (under the supervision of M. Kleiber), IFTR, Warsaw, PL, (in polish)

13. POSTEK E., HANGANU A., OÑATE E., BARBAT A.H., 1994, Failure analysis of nuclear reactor containment shells, *30^{th} Polish Conference on Solid Mechanics, Conference Abstracts*, Zakopane, September

14. POSTEK E., KLEIBER M., 1996, Parameter sensitivity of RC shell structures, in: *Prof. Z. Kączkowski Jubilee Volume*, Warsaw University of Technology, Warsaw, 345-358, (in polish)

15. RACKWITZ R., FIESSLER B., 1978, Structural reliability under combined load sequences, *Computers and Structures*, **9**, 489-494

16. SANTOS J.L.T., SIEMASZKO A., GOLLWITZER S., RACKWITZ R., 1995, Continuum sensitivity method for reliability-based structural design and optimization, *Mech. Struct. and Mach.*, **23**, 497-520

17. SIEMASZKO A., SANTOS J.L.T., 1993, Reliability-based structural optimization, *Proc. Struct. Opt. 93 World Congress*, Rio de Janeiro, I, 473-480

18. Abaqus, Theory and User's Manual, version 6.12

19. COMREL-TI, User's Manual, Reliability Consulting Programs GmbH, Barer Str. 48, Munich, GE., 1992

20. Nastran manuals, MSC Nastran

Analiza niezawodności osłony budynku reaktora

Streszczenie

Analiza niezawodności dużych konstrukcji wymaga zazwyczaj bardzo długich obliczeń komputerowych. Poprawa efektywności algorytmów jest zazwyczaj warunkiem koniecznym uzyskania rozwiązań dla dużych rzeczywistych problemów. Analizę niezawodności zwykle przeprowadza się stosując przybliżoną metodę analizy niezawodności pierwszego rzędu (FORM). Procedury iteracyjne analizy niezawodności pierwszego rzędu (FORM) wymagają obliczenia gradientów wrażliwości o wysokiej dokładności. Projektowanie konstrukcji wymaga stosowania metod numerycznych takich jak metoda elementów skończonych. Gradienty wrażliwości nie są jawnie zależne od zmiennych projektowych. Obliczenia gradientów wrażliwości powinno być realizowane przy zastosowaniu efektywnych, dyskretnych metod analizy wrażliwości. W artykule przedstawiono sposób połączenia analizy niezawodności z dyskretnymi metodami obliczania gradientów wrażliwości – zmiennej sprzężonej (AVM) i różniczkowania bezpośredniego (DDM). Rozwinięty program komputerowy dla żelbetowych powłok warstwowych pozwala na rozwiązywanie dużych zadań niezawodnościowych. Przedstawiona została analiza niezawodności żelbetowego budynku bezpieczeństwa reaktora nuklearnego. Analiza niezawodności pozwala na stwierdzenie, który z parametrów projektowych ma największy wpływ na niezawodność osłony.

Manuscript received October 2, 2001; accepted for print November 12, 2001